Simulation and Analysis of NMR Lines Reflecting the Chemical Shift Anisotropy for the Characterization of Local Motions of Glassy Polymers (Commemoration Issue Dedicated to Professor Hisashi Odani On the Occasion of His Retirement)

AUTHOR(S):

Horii, Fumitaka; Uyeda, Tadashi; Beppu, Takayuki; Murata, Tsuyoshi; Odani, Hisashi

CITATION:

Horii, Fumitaka ...[et al]. Simulation and Analysis of NMR Lines Reflecting the Chemical Shift Anisotropy for the Characterization of Local Motions of Glassy Polymers (Commemoration Issue Dedicated to Professor Hisashi Odani On the Occasion of His Retirement). Bulletin of the Institute for Chemical Research, Kyoto University 1992, 70(2): 198-212

ISSUE DATE:

1992-09-30

URL:

http://hdl.handle.net/2433/77443

Bull. Inst. Chem. Res., Kyoto Univ., Vol. 70, No. 2, 1992

Simulation and Analysis of NMR Lines Reflecting the Chemical Shift Anisotropy for the Characterization of Local Motions of Glassy Polymers

Fumitaka HORII*, Tadashi UYEDA*, Takayuki BEPPU*, Tsuyoshi MURATA*, and Hisashi ODANI*

Received July 7, 1992

In an attempt of the characterization of local motions of glassy polymers, we have derived considerably general equations for NMR lines reflecting chemical shift anisotropies using *N*-site exchange models. As for two characteristic motions, flip motions of a phenyl ring and the orientational fluctuation of a rotation axis, resonance lines of specific nuclei associated with these motions have been simulated as functions of the flip angle or the amplitude of the fluctuation as well as of exchange frequency. The comparison of these simulated spectra is simply made with the corresponding ^{13}C powder spectra of the aromatic CH carbon of bisphenol A polycarbonate, which have been obtained by selective excitation switching angle sample spinning (SASS) NMR, and with ^{29}Si powder spectra of polyacetylene derivatives containing trimethylsilyl groups.

KEYWORDS: Simulation of NMR Lines / *N*-Site Exchange Models / Chemical Shift Anisotropy / Molecular Motion / Glassy Polymers / Polycarbonates / Polyacetylene Derivatives / Selective Excitation SASS NMR

INTRODUCTION

For a number of reasons, the structure and molecular motions of glassy polymers are of great interest. From an application viewpoint, the mechanical and thermal properties as well as gas permeabilities strongly depend on the structure and dynamics of the glassy state. Over the past 30 years the local chain dynamics of glassy polymers has been investigated by different experimental methods including dielectric relaxation, dynamic mechanical relaxation, NMR relaxation measurements. Although those studies did provide useful information about secondary transitions which are thought to arise from specific types of local motion, the structural specification of each motion was frequently unsuccessful in those traditional relaxation experiments.

Recently, more sophisticated solid-state ^{13}C NMR has been developed by combining the dipolar decoupling (DD) and cross polarization with or without magic angle spinning (MAS).[1] Since this method allows us to obtain spin relaxation parameters and line shapes

* 堀井文敬, 植田 正, 別府隆幸, 村田ツヨシ, 小谷 壽:
Laboratory of Fundamental Material Properties, Institute for Chemical Research, Kyoto University, Uji, Kyoto 611, Japan

reflecting chemical shift anisotropies[2,3] and ^{13}C-^{1}H dipolar interaction[4-6] for the individual carbons, we can characterize the detailed local motions of glassy polymers by analyzing the parameters and line shapes with the use of appropriate models for molecular motions. For example, we have analyzed ^{13}C spin-lattice relaxation times (T_{1C}) of α-methyl carbons of poly(methyl methacrylate)s with different tacticities and also T_{1C}s of methyl carbons of bisphenol A polycarbonate (BPAPC),[8] poly(1-trimethylsilyl-1-propyne) (PMSP)[9] and poly(*o*-trimethylsilyl phenyl acetylene) (PTPA),[9] and found a three-fold rotation with frequencies ranging from 10^7 to 10^{11} Hz and a rapid fluctuation in picoseconds around the potential minima for the rotation in their glassy state.

In this paper we first derive a considerably general equation for a resonance line reflecting the chemical shift anisotropy by use of N-site exchange models. Using this equation some typical resonance lines are simultated for the cases of 180° or restricted jump rotations of a phenyl ring and a spacial fluctuation of the rotation axis associated with side groups such as a methyl group and trimethylsilyl group. Those simulated spectra are also compared with experimental spectra for the natural abundant ortho ^{13}C nucleus of the phenyl ring in BPAPC and for the ^{29}Si nucleus of the trimethylsilyl group in PMSP and PTPA. Here, the former ^{13}C NMR spectrum has been obtained by the selective excitation switching angle sample spinning (SASS)[10,11] method, which includes the use of the DANTE pulse sequence[12,13] and a Doty dynamic angle spinning (DAS)[14] probe, on the basis of the version previously proposed.[15]

THEORETICAL

In a homonuclear spin system, where each spin is distributed at N-sites at an equal probability and jumps randomly among these sites at the same frequency $\varkappa$, the resonance line $I(\omega)$ is given by[16]

$$I(\omega)=N^{-1}\mathrm{Re}\,[L/(1-\varkappa L)] \tag{1}$$

where

$$L=\sum_{j=1}^{N}\,[\mathrm{i}\,(\omega-\omega_j)+N\varkappa]^{-1} \tag{2}$$

Here, ω_j is the resonance frequency at site j. For $N=2$, eq. (1) reduces to a well-known equation for a two-site exchange model;[16,17]

$$I(\omega)=\frac{1}{2}\,\frac{\varkappa\,(\omega_1-\omega_2)^2}{(\omega-\omega_1)^2(\omega-\omega_2)^2+\varkappa^2[2\omega-(\omega_1+\omega_2)]^2} \tag{3}$$

Moreover, after a tedious calculation, we obtain the following equation for $N=4m$, where m is the positive integer.

$$I(\omega)=(1/4m)\,(ac+bd)\,/\,(a^2+b^2) \tag{4}$$

Here

$$
\begin{aligned}
a&=\Omega_{4m}+\chi\sum_{j=1}^{2m}(-1)^j\,(4m-2j)\,(4m\chi)^{2j-1}\Omega_{4m-2j}\\
b&=\chi\sum_{j=1}^{2m}(-1)^j\,(4m-2j+1)\,(4m\chi)^{2j-2}\Omega_{4m-2j+1}\\
c&=\sum_{j=1}^{2m}(-1)^j\,(2j)\,(4m\chi)^{2j-1}\Omega_{4m-2j}\\
d&=\sum_{j=1}^{2m}(-1)^j\,(2j-1)\,(4m\chi)^{2j-2}\Omega_{4m-2j+1}
\end{aligned}
\tag{5}
$$

and

$$
\begin{aligned}
\Omega_0&=1\\
\Omega_1&=(\omega-\omega_1)+(\omega-\omega_2)+\cdots\cdots+(\omega-\omega_N)\\
\Omega_2&=(\omega-\omega_1)\,(\omega-\omega_2)+(\omega-\omega_1)\,(\omega-\omega_3)+\cdots\cdots\\
&\quad+(\omega-\omega_2)\,(\omega-\omega_3)+(\omega-\omega_2)\,(\omega-\omega_4)+\cdots\cdots\\
&\quad\cdots\cdots\\
&\quad+(\omega-\omega_{N-1})\,(\omega-\omega_N)\\
\Omega_3&=(\omega-\omega_1)\,(\omega-\omega_2)\,(\omega-\omega_3)+(\omega-\omega_1)\,(\omega-\omega_2)\,(\omega-\omega_4)+\cdots\cdots\\
&\quad+(\omega-\omega_2)\,(\omega-\omega_3)\,(\omega-\omega_4)+\cdots\cdots\\
&\quad\cdots\cdots\\
&\quad+(\omega-\omega_{N-2})\,(\omega-\omega_{N-1})\,(\omega-\omega_N)\\
&\quad\cdots\cdots\cdots\\
\Omega_N&=(\omega-\omega_1)\,(\omega-\omega_2)\cdots\cdots(\omega-\omega_N)
\end{aligned}
\tag{6}
$$

However, it may be much easier in the case of larger N to numerically calculate lineshapes $I(\omega)$ by the rationalization with the aid of a computer. Eq. (1) is applicable to the calculation of different resonance lines reflecting the quadrupolar interaction, ^{13}C-^{1}H dipolar interaction, chemical shift anisotropies and so on. In this paper, however, we treat the case of the chemical shift anisotropy using appropriate models of molecular motion.

When the shielding Hamiltonian $\mathcal{H}_s$ in the laboratory frame is represented in the irreducible spherical tensor notation, the secular part of this interaction is given by[16,18]

$$
\mathcal{H}_s=A_{00}^{L}\,T_{00}^{L}+A_{20}^{L}\,T_{20}^{L} \tag{7}
$$

with

$$
\begin{aligned}
A_{00}^{L}&=-\mathrm{Tr}(\sigma_{ij}^{L})/\sqrt{3}, \quad A_{20}^{L}=[3\sigma_{zz}^{L}-\mathrm{Tr}(\sigma_{ij}^{L})]/\sqrt{6}\\
T_{00}^{L}&=-\gamma_I B_0 I_z/\sqrt{3}, \quad T_{20}^{L}=(2/\sqrt{6})\gamma_I B_0 I_z
\end{aligned}
\tag{8}
$$

Here, γ_I is the gyromagnetic ratio for a nucleus I, σ_{ij}^{L} is the ij component of the second-rank chemical shift tensor in the laboratory frame, B_0 is the strength of the static magnetic field, and I_z is the component along the static magnetic field (z axis) for spin operator $\boldsymbol{I}$. Accordingly, the resonance frequency ω_j for site j will be expressed as

$$\omega_j = \omega_I + \omega'_j \tag{9}$$

where

$$\omega_I = \gamma_I B_0 \mathrm{Tr}(\sigma^L_{ij}) / 3 = \omega_0 \mathrm{Tr}(\sigma_{ij}) / 3 \tag{10}$$

$$\omega'_j = (2/\sqrt{6})\gamma_I B_0 A^L_{20} = (2/\sqrt{6})\omega_0 A^L_{20} \tag{11}$$

In eq. (10) σ^L_{ij} can be replaced by the ij component σ_{ij} of the chemical shift tensor in the principal axis system, because the trace Tr (σ_{ij}) is invariant upon the orthogonal coordinate transformation. On the other hand, the component A^L_{20} of the irreducible tensor in eq. (11) will be described in terms of the components of the corresponding tensor A in the principal axis frame using appropriate orthogonal transformations. Such coordinate transformations should depend on the molecular motion of a sequence or a side-group in which a nucleus in question is involved.

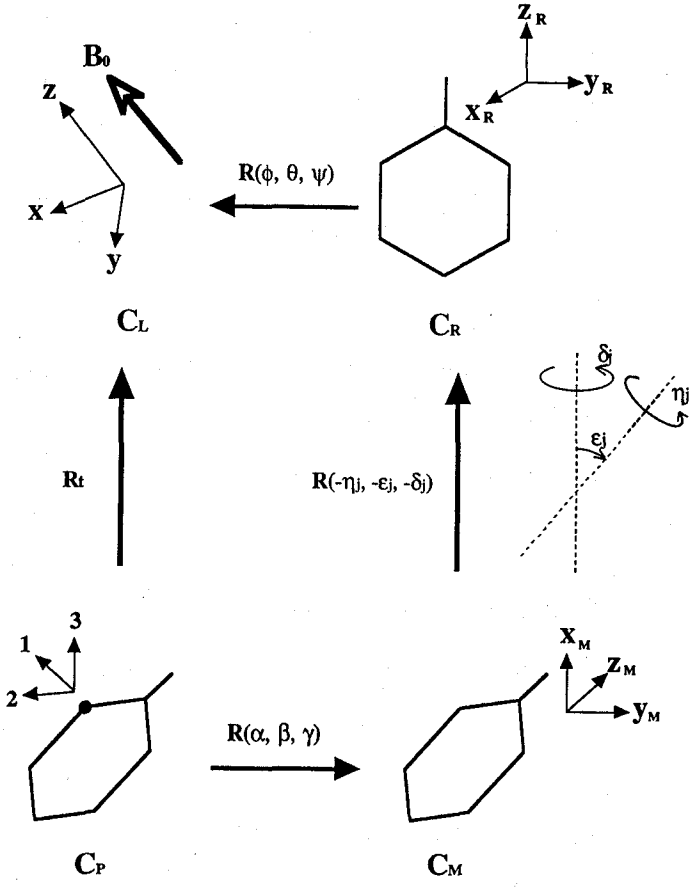

Fig. 1. Schematic representation of the coordinate transformation from the principal axis system (C_P) through the molecular frame (C_M) and the reference frame (C_R) to the laboratory frame (C_L).

In Figure 1 a series of coordinate transformations are schematically shown for the case of the ortho carbon in the phenyl group. Here, we first define the molecular frame (C_M) as follows; the z_M axis is set along the single bond of the quaternary carbon, while the x_M axis is perpendicular to the plane of the phenyl ring. When the molecular frame in the rigid state is defined as the reference frame (C_R), the molecular frame located at site j will be described in terms of Eulerian angles (δ_j, ε_j, η_j) in the reference frame. Moreover, the molecular frame at site j may be correlated to the principal axis system (C_P) for the ortho carbon using another set of Eulerian angles (α, β, γ). Here, the principal axis system may be oriented with the σ_{11} axis parallel to the C-H bond and the σ_{33} axis perpendicular to the ring plane, as reported for benzene.[16] On the other hand, the laboratory frame can be also described in terms of Eulerian angles (ϕ, θ, ψ) in the reference frame in a similar manner. Finally we can correlate the principal axis system with the laboratory frame using the following coordinate transformations:

$$C_P \xrightarrow{R(\alpha,\beta,\gamma)} C_M \xrightarrow{R(-\eta_j,-\varepsilon_j,-\delta_j)} C_R \xrightarrow{R(\phi,\theta,\psi)} C_L$$

The total transformation matrix R_t is given by

$$R_t=R(\phi,\theta,\psi)\,R(-\eta_j,-\varepsilon_j,-\delta_j)\,R(\alpha,\beta,\gamma) \tag{12}$$

Using this transformation matrix, A_{20}^L in eq. (11) is described in terms of the components of the corresponding tensor A in the principal axis system:

$$A_{20}^L=R_tA_{20}R_t^{-1} \tag{13}$$

Since the unitary transformation of a spherical tensor is also expressed in terms of the Wigner rotation matrices, eq. (13) reduces to

$$A_{20}^L=\sum_{p,q,r=-2}^{2} A_{2r}D_{rq}^2(\alpha,\beta,\gamma)\,D_{qp}^2(-\delta_j,-\varepsilon_j,-\eta_j)D_{p0}^2(\phi,\theta,\psi) \tag{14}$$

or

$$\begin{aligned}A_{20}^L=&\sum_{p,q,r=-2}^{2} A_{2r}d_{rq}^2(\beta)d_{qp}^2(-\varepsilon_j)d_{p0}^2(\theta)\\&\times\exp(-\mathrm{i}\alpha r)\exp[-\mathrm{i}(\gamma-\eta_j)q]\exp[-\mathrm{i}(\phi-\delta_j)p]\end{aligned} \tag{15}$$

where $d_{ij}^2(\theta)$ are given in Table B. 1. in Ref. (16). A_{2r} are represented according to their definition as

$$\begin{aligned}&A_{20}=(\sqrt{6}/2)\,[\sigma_{33}-\mathrm{Tr}(\sigma_{ij})/3]\equiv(\sqrt{6}/2)\sigma_{33}{}^*\\&A_{2\pm1}=0\\&A_{2\pm2}=(\sigma_{11}-\sigma_{22})/2\end{aligned} \tag{16}$$

As a consequence, one can obtain the following equation for ω'_j in eq. (11):

$$\begin{aligned}\omega'_j=&(3/16)\omega_0\sigma_{33}{}^*\ [C_1\sin^2\beta\sin^2\theta-2C_2\sin2\beta\sin\varepsilon_j\sin^2\theta\\&-2C_3\sin^2\beta\sin\varepsilon_j\sin2\theta-2C_4\sin2\beta\sin2\theta\\&+4P(\beta)\sin\varepsilon_j\sin\theta(\sin\varepsilon_j\sin\theta\cos2\Phi_j+4\cos\varepsilon_j\cos\theta\cos\Phi_j)\\&+4P(\theta)\sin\beta\sin\varepsilon_j(\sin2\beta\cos2\Lambda_j\sin\varepsilon_j+4\cos\beta\cos\Lambda_j\cos\varepsilon_j)\\&+(16/3)P(\beta)P(\varepsilon_j)P(\theta)]\\&+\omega_0(\sigma_{11}-\sigma_{22})\{\sin^2\theta[C_1\cos2\alpha(1+\cos^2\beta)/2-S_1\sin2\alpha\cos\beta]\\&+2\sin\beta\sin\varepsilon_j\sin^2\theta(C_2\cos2\alpha\cos\beta-S_2\sin2\alpha)\\&-\sin\varepsilon_j\sin2\theta[C_3\cos2\alpha(1+\cos^2\beta)-2S_3\sin2\alpha\cos\beta]\\&+2\sin\beta\sin2\theta(C_4\cos2\alpha\cos\beta-S_4\sin2\alpha)\\&+3\cos2\alpha\sin^2\beta\sin\varepsilon_j\sin\theta(\sin\varepsilon_j\sin\theta\cos2\Phi_j+4\cos\varepsilon_j\cos\theta\cos\Phi_j)\\&+2P(\theta)\sin^2\varepsilon_j[\cos2\alpha(1+\cos^2\beta)\cos2\Lambda_j-2\sin2\alpha\cos\beta\sin2\Lambda_j]\\&-4P(\theta)\sin\beta\sin2\varepsilon_j(\cos2\alpha\cos\beta\cos\Lambda_j-\sin2\alpha\sin\Lambda_j)\\&+4P(\varepsilon_j)P(\theta)\cos2\alpha\sin^2\beta\}/8\end{aligned}\tag{17}$$

Here

$$P(\theta)=(3\cos^2\theta-1)/2\tag{18}$$

$$\Lambda_j=\gamma-\eta_j\tag{19}$$

$$\Phi_j=\phi-\delta_j\tag{20}$$

$$\begin{aligned}C_1&=E_1{}^2\cos(2\Lambda_j+2\Phi_j)+E_2{}^2\cos(2\Lambda_j-2\Phi_j)\\C_2&=E_1\cos(\Lambda_j+2\Phi_j)-E_2\cos(\Lambda_j-2\Phi_j)\\C_3&=E_1\cos(2\Lambda_j+\Phi_j)-E_2\cos(2\Lambda_j-\Phi_j)\\C_4&=E_1E_4\cos(\Lambda_j+\Phi_j)-E_2E_3\cos(\Lambda_j-\Phi_j)\end{aligned}\tag{21}$$

$$\begin{aligned}S_1&=E_1{}^2\sin(2\Lambda_j+2\Phi_j)+E_2{}^2\sin(2\Lambda_j-2\Phi_j)\\S_2&=E_1\sin(\Lambda_j+2\Phi_j)-E_2\sin(\Lambda_j-2\Phi_j)\\S_3&=E_1\sin(2\Lambda_j+\Phi_j)-E_2\sin(2\Lambda_j-\Phi_j)\\S_4&=E_1E_4\sin(\Lambda_j+\Phi_j)-E_2E_3\sin(\Lambda_j-\Phi_j)\end{aligned}\tag{22}$$

$$\begin{aligned}E_1&=\cos\varepsilon_j+1\\E_2&=-\cos\varepsilon_j+1\\E_3&=2\cos\varepsilon_j+1\\E_4&=2\cos\varepsilon_j-1\end{aligned}\tag{23}$$

Using eq. (17), we can calculate the resonance frequency ω'_j for site j which is defined by Eulerian angles (δ_j, ε_j, η_j). In real samples there should appear some distributions in Eulerian angles ϕ and θ depending on the orientation of molecules. When the orientation is completely random, $I(\omega)$ given by eq. (1) should be averaged as follows:

$$I_{pw}(\omega)=(1/4\pi)\int_0^{2\pi}d\phi\int_0^{\pi}I(\omega)\sin\theta d\theta \tag{24}$$

In this paper resonance lines are simulated for the following two cases.

(1) Flip Motions of the Phenyl Ring.

The phenyl ring frequently undergoes flip motions such as 180°-jump rotation even in the glassy state. Since the principal axis system of the ortho carbon is defined as shown in Figure 1, one can determine α, β and γ in eq. (17) as follows; $\alpha=2\pi/3$, $\beta=-\pi/2$, and $\gamma=0$. Moreover, in the two-site exchange model $\eta_1=\varepsilon_1=\delta_1=0$ for site $j=1$, and $\eta_2=\varepsilon_2=0$ and $\delta_2=\delta$ for site $j=2$, δ being the flip angle. Accordingly, eq. (17) reduces to

$$\begin{aligned}\omega'_1=&\omega_0\sigma_{33}^*\,(3\cos2\phi\sin^2\theta-3\cos^2\theta+1)/4\\&-\omega_0(\sigma_{11}-\sigma_{22})[\sin^2\theta\cos2\phi\\&+2\sqrt{3}\sin2\theta\sin\phi+3\cos^2\theta-1]/8\end{aligned} \tag{25}$$

$$\begin{aligned}\omega'_2=&\omega_0\sigma_{33}^*\,[3\cos2(\phi-\delta)\sin^2\theta-3\cos^2\theta+1]/4\\&-\omega_0(\sigma_{11}-\sigma_{22})[\sin^2\theta\cos2(\phi-\delta)\\&+2\sqrt{3}\sin2\theta\sin(\phi-\delta)+3\cos^2\theta-1]/8\end{aligned} \tag{26}$$

(2) Orientational Fluctuation of a Rotation Axis.

As will be described later, the rotation axis of the CH_3 group in BPAPC or the trimethylsilyl group in PMSP may undergo a restricted fluctuation in orientation as a result of the local motion of backbone carbons. We analyze this kind of motion using an N-site jump model where the rotation axis (the C-X axis) fluctuates among N sites with a frequen-

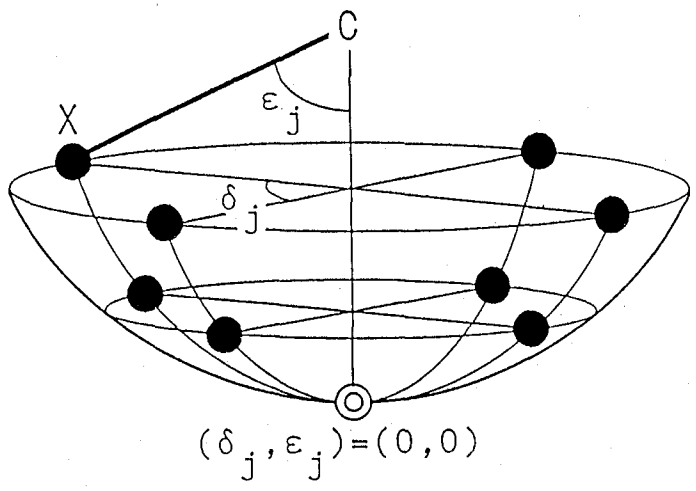

Fig. 2. Schematic representation of the respective sites for the fluctuation of the rotation axis C-X in an N-site jump model.

cy κ, as shown in Figure 2. Assume that each site, which is described in terms of angles (δ_j, ε_j), is located on a surface of a sphere whose radius corresponds to the bond length of the rotation axis. In the rigid state the rotation axis remains at site (0, 0). In this case the z axis of the reference frame (C_R), which is described in Figure 1, is set along the C-X axis. Since the rotation about the C-X axis is assumed to be fully rapid, the x or y axis of C_R is simply defined as a certain axis perpendicular to the C-X axis. Then angles δ_j and ε_j correspond to Eulerian angles δ_j and ε_j shown in Figure 1. Since one can set any value for η_j because of the rapid rotation about the C-X axis, η_j should be zero in this model. On the other hand, the principal axis system is in accord with the molecular frame according to the spectra of the CH_3 carbon of BPAPC[8] and ^{29}Si nucleus of PMSP[9], resulting in $\alpha=\beta=\gamma=0$. Since σ_{11} should be equal to σ_{22} owing to the rapid rotation about the σ_{33} axis (the C-X axis), eq. (17) reduce to

$$\omega'_j=\omega_0\sigma_{33}{}^*[3\sin^2\varepsilon_j\sin^2\theta\cos(2\phi-2\delta_j)+\sin2\theta\sin2\varepsilon_j\cos(\phi-\delta_j)+(3\cos^2\varepsilon_j-1)(3\cos^2\theta-1)]/4 \quad (27)$$

being as a function of ε_j and δ_j.

EXPERIMENTAL

Samples. Bisphenol A polycarbonate pellets, which were provided by Teijin Chemicals, Ltd., were hot-pressed at 320°C under 150 kg/cm^2 and quenched in iced water. This sample was stored in a glass tube at about 4°C in a refrigerator before NMR measurements.

PMSP and PTPA films were prepared on a clean mercury surface by prolonged solvent-casting at room temperature. Each film was then immersed in methanol at least for 7 days and dried under vacuum for about 2 days.

NMR Measurements. ^{13}C and ^{29}Si NMR measurements were performed on JEOL JNM-GX200 and JNM-GX400 spectrometers operating under static magnetic fields of 4.7 and

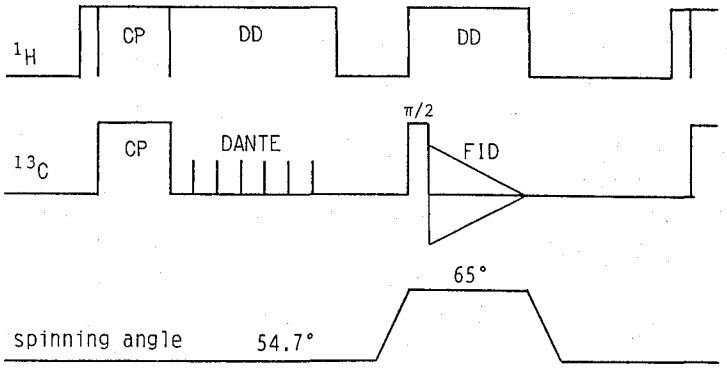

Fig. 3. Pulse diagram for selective excitation switching angle sample spinning NMR to obtain a chemical shift anisotropy powder pattern in a one-dimensional experiment.

9.4T, respectively. Selectively excited ^{13}C NMR spectra reflecting the chemical shift anisotropies were obtained by combining the cross polarization, DANTE pulse sequence, and the switching angle sample spinning,[15] as shown in Figure 3, with the use of a DAS probe purchased from Doty Scientific, Inc. The matched ^{1}H and ^{13}C field strengths $\gamma B_1/2\pi$ were 59.5 kHz in the CP process and the rate of sample spinning was 3.5 kHz. During the DANTE sequence, a ^{13}C radio frequency attenuator was used to increase the selectivity of the DANTE sequence. The DANTE $\pi/2$ pulse sequence consisted of a train of 10 pulses spaced by 283 μs, each consitituent pulse length being 2.4μs. ^{29}Si powder spectra were obtained by the CP technique without MAS using a JEOL VT/MAS probe equipped to a JNM-GX400 spectrometer. The matched ^{1}H and ^{29}Si field strengths were 44.6-50.0 kHz.

RESULTS AND DISCUSSION

1. Simulation of Resonance Lines.

Flip motions of the phenyl ring with different flip angles δ.

Figure 4 shows ^{13}C NMR resonance lines simulated by using eqs. (3) and (24)-(26) for the ortho carbon in the phenyl ring when the ring undergoes the flip motions with different flip angles δ and reduced rates κ' ($=10^6\kappa/\omega_0$). Here, σ_{11}, σ_{22}, and σ_{33} values are assumed to be 204, 152, and 29 ppm,[2] respectively, being independent on the flip angle. Each resonance line was convoluted in terms of a Lorentzian curve with the linewidth of 5 ppm.

Marked changes in line shape can be recognized for δ values more than 30° when κ' values are of the order of 1-100; a typical powder pattern reflecting different σ_{11}, σ_{22}, and σ_{33} values narrows in different ways with increasing κ', strongly depending on the flip angle. In particular, the simulated line for $\delta=90°$ and $\kappa'=100$ possesses a characteristic shape possibly as a result of a rapid exchange between the σ_{11}-σ_{22} plane (the benzene ring plane) and the plane including the σ_{33} axis. Such a 90° flip motion also seems to produce the narrowest line width in this case. In contrast, the line shape for the 180° flip motion is not subjected to a large change even for higher κ' values; some appreciable average seems to occur between the σ_{11} and σ_{22} contributions, while the σ_{11} component stays almost constant. This must stem from the motional average by the exchanges between the σ_{11} and σ_{22} axis and between the σ_{33} and $-\sigma_{33}$ axis, which are induced by the 180° flip motion.

Orientational fluctuation of the rotation axis.

Figure 5 shows powder spectra of the nucleus X simulated by using eqs. (1), (24), and (27) for different ε and κ' values at $\delta=360/4$, when the rotation axis C-X fluctuates in orientation as shown in Figure 2. Here, each δ value is described as a fraction in which the numerator and denominator indicate the maximum ε_j value, which corresponds to the maximum amplitude of the fluctuation, and the number m of sites along the direction associated with angle ε_j, respectively. In a similar fashion δ is also expressed as 360/4, indicating that the number of sites along the δ_j direction is 4 and thus $\delta_j=0$, 90, 180, and 270°. The total number N of sites is, therefore, assumed to be $4m+1$. Moreover, it has been assumed that $\sigma_{11}=\sigma_{22}=0$ ppm and $\sigma_{33}=-30$ ppm in this case. The convolution of a Lorentzian curve with a linewidth of 2 ppm was also conducted for each simulated resonance line $I_{pw}(\omega)$ in eq. (24).

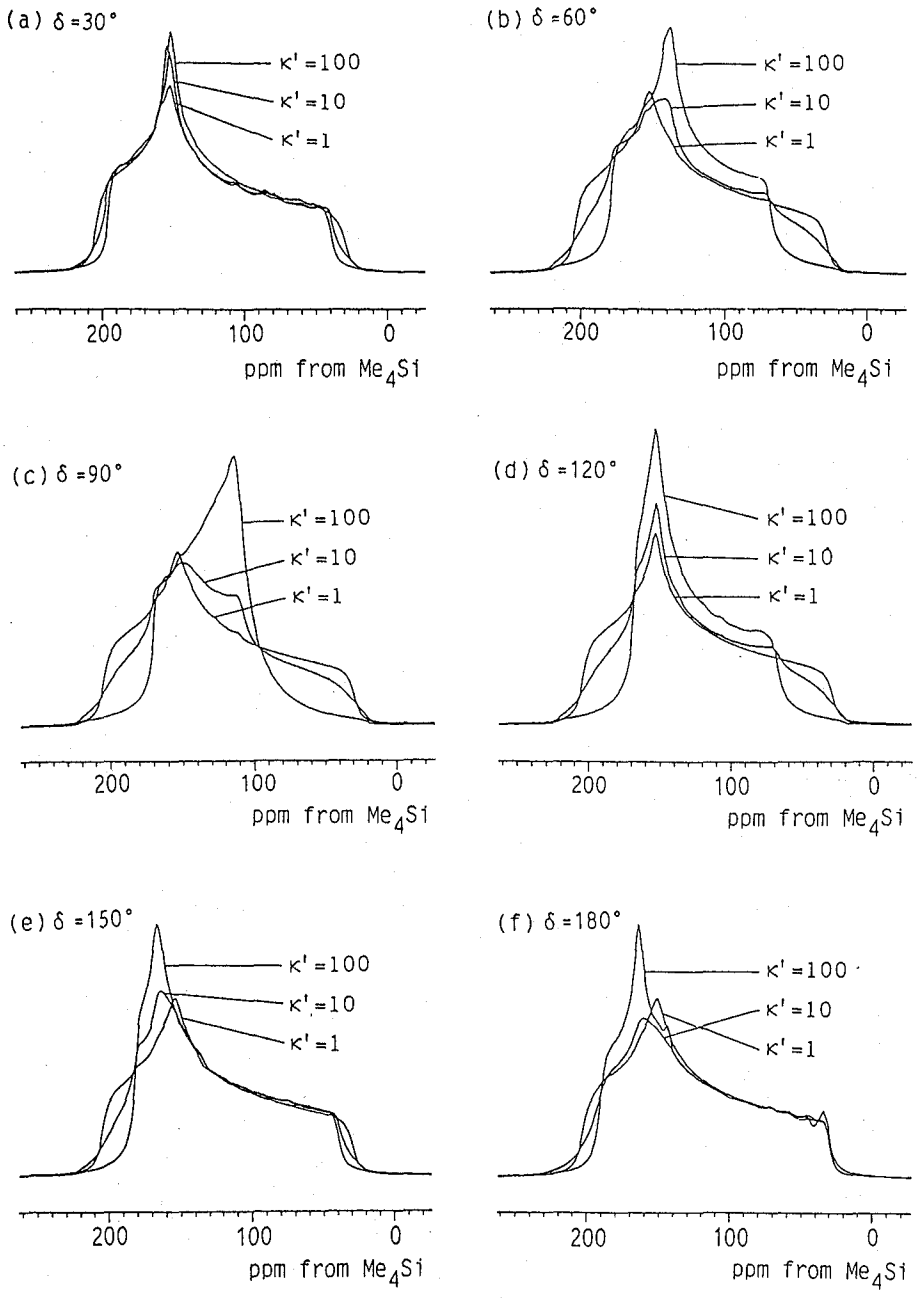

Fig. 4. Powder spectra simulated for the ortho carbon of the phenyl group which undergoes flip motions with different flip angles δ, using a two-site exchange model.

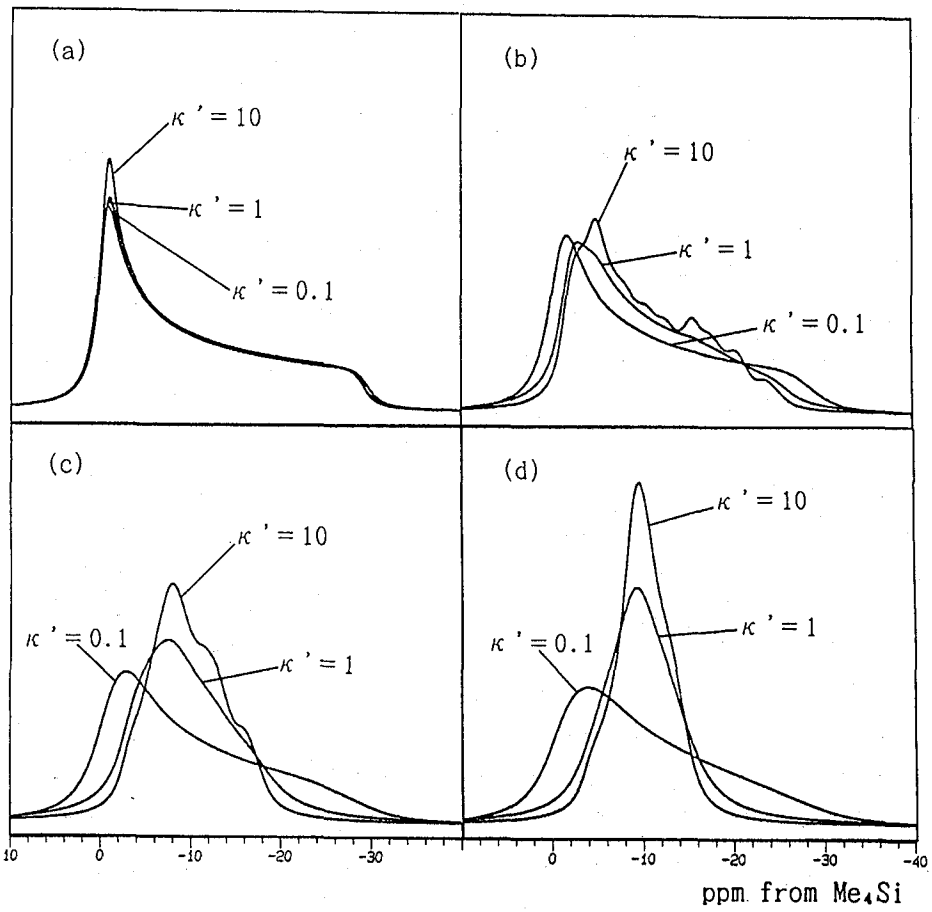

Fig. 5. Powder spectra simulated for the nucleus X in the fluctuation of the rotation axis C-X as shown in Figure 2 with different κ' and ε values at δ=360/4. (a) ε=15/3, (b) ε=30/6, (c) ε=45/9, (d) ε=60/12.

When the maximum ε_j value is less then 15°, the simulated lines are very close to the axially symmetric powder spectrum in the rigid state even for higher κ' values. However, the narrowing evidently begins to occur at ε=30/6 with increasing κ' values. For larger ε values the lines become further narrower and an almost Lorentzian line is obtained for ε =60/12 and κ'=10. The latter result indicates that the rotation axis may undergo a fluctuation with the amplitude more than 60°, when a Lorentzian resonance line is experimentally observed. In this case the frequency of the fluctuation will be estimated to be higher than 10^3 Hz if the resonance frequency of 100 MHz is employed for the measurement.

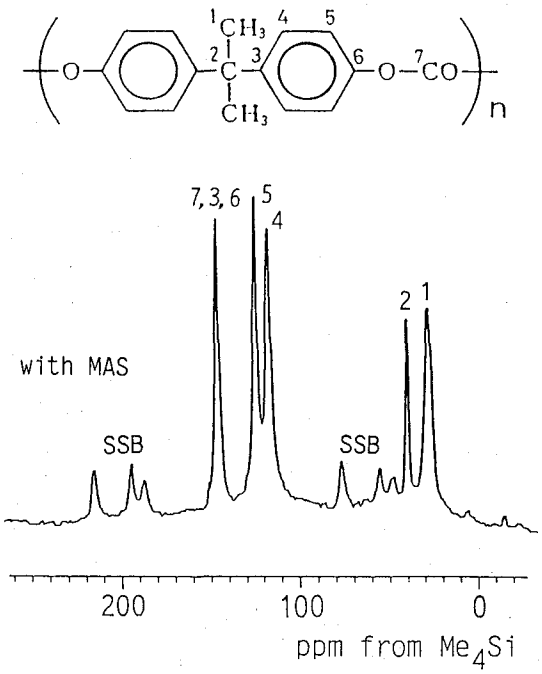

Fig. 6. 50 MHz CP/MAS ^{13}C NMR spectrum of bisphenol A polycarbonate (BPAPC) measured at room temperature.

2. Experimentally Observed Resonance Lines.

In order to compare the simulated resonance lines described above with the corresponding experimental spectra, we have measured two examples shown below. Figure 6 shows 50 MHz CP/MAS ^{13}C NMR spectrum of BPAPC measured at room temperature. Each resonance line has been assigned to each carbon of BPAPC in analogy with the assignment of the solution-state spectrum which was made by the 2D INADEQUATE method. It should be noted here that the previous assignment[19] for C4 and C5 carbons must be revised according to our new assignment.

Figure 7 shows chemical shift anisotropy powder spectra for the C5 carbon of BPAPC, which were obtained at different temperatures by selective excitation SASS method and reproduced by considering the scaling factor $(3\cos^2\zeta\text{-}1)/2$ for the sample spinning at an angle ζ. 1000-1500 free induction decays were accumulated in those cases. The selective observation of the C5 carbon seems successful under conditions set for the DANTE pulse sequence described above.

The observed spectra, which seem to resemble axially symmetric lines, significantly differ from the simulated spectra for the 180° jump rotation shown in Figure 4. Roy and Jones[3] analyzed similar spectra for the identical carbon of BPAPC, which were obtained for the selectively ^{13}C-enriched sample, by using an N-site exchange model. In this case flip motions were assumed to be induced among 22 sites located around two conformational minima separated by 180°, and thus there were jumps of $180° \pm m\theta$ as well as $m\theta$ where m was the integer less than 6 and θ is 4.6-12.8° at −80-120°C. However, the flips with angles

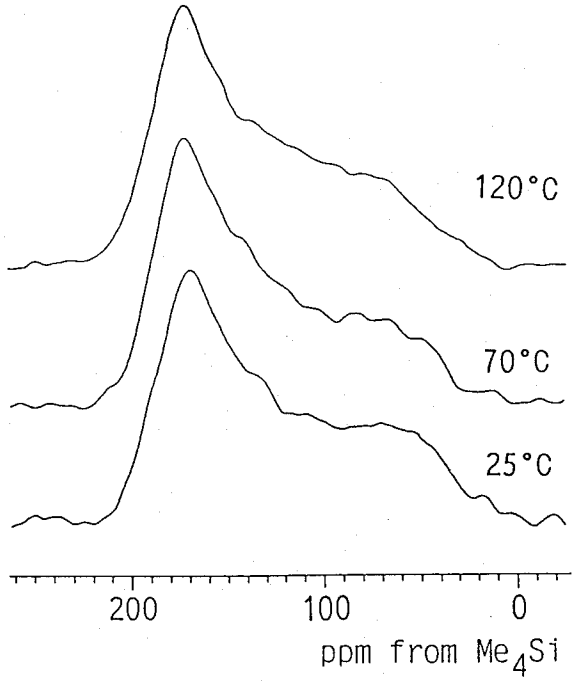

Fig. 7. Chemical shift anisotropy powder spectra of the C5 carbon of BPAPC, which were obtained by selective excitation SASS NMR at different temperatures.

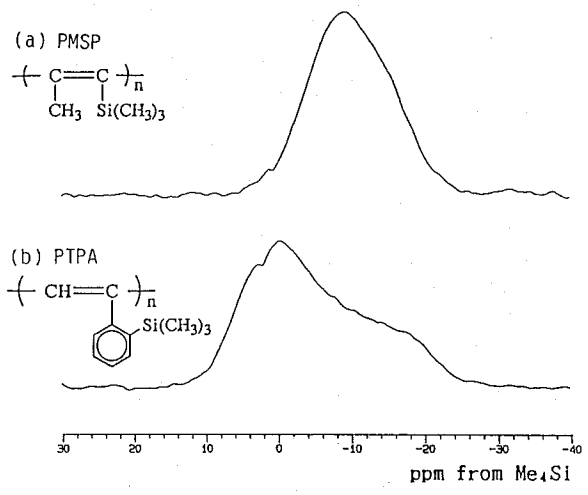

Fig. 8. CP/DD ^{29}Si NMR spectra obtained for PMSP and PTPA without MAS at room temperature.

less than 30° should not contribute the change in line shape as shown in Figure 5(a). Moreover, the spectrum (Figure 5(e)) simulated for $\delta=150°$ and $\kappa'=100$ is rather similar to the observed resonance lines. These suggest that the distribution in flip angle around 180° should be considered together with the distribution in κ'. Further analyses are in progress in order to clarify the effects of these distributions.

Figure 8 shows CP/DD ^{29}Si NMR spectra obtained for PMSP and PTPA without MAS at room temperature. The spectrum of PTPA seems axially symmetric, whereas the resonance line of PMSP is almost narrowed. This suggests that the C-Si bond, connecting the backbone carbon with the Si nucleus in the trimethylsilyl group, is highly resticted for PTPA in the orientational fluctuation described above, while such fluctuation may be considerably enhanced for PMSP.

In the separate analysis of ^{13}C spin-lattice relaxation times for the CH_3 group of PMSP, it has been found that the rotation about the C-Si bond is as high as about 10^8 Hz at room temperature.[9] Accordingly, we can examine the fluctuation of the C-Si bond of PMSP by using the *N*-site exchange model based on eq. (27). The comparison of the experimental spectrum with the simulated spectra shown in Figure 5 has revealed that the former spectrum well corresponds to the line shape simulated for $\varepsilon=45/9$, $\delta=360/4$ and $\kappa'=1$. This indicates that the C-Si bond of PMSP undergoes the orientational fluctuation with the amplitude of about 45° and the frequency of the order of 10^2 Hz. It should be noted that such a high amplitude motion associated with the backbone carbon could be allowed in the glassy state. Further discussion will be made somewhere after the measurement of ^{13}C chemical shift anisotropy for backbone carbons of PMSP using selective excitation SASS NMR.

ACKNOWLEDGMENT

We are very grateful to Professor Toshinobu Higashimura and Dr. Toshio Masuda of Department of Polymer Chemistry, Kyoto University, for providing different polyacetylene derivatives.

REFERENCES

1) For example, see "Solid State NMR of Polymers", L.J. Mathias, Ed., Plenum Press, New York and London, 1991.
2) J.F. O'Gara, A.A. Jones, C.-C. Hung, and P.T. Inglefield, *Macromolecules*, **18**, 1117 (1985).
3) A.K. Roy and A.A. Jones, *J. Magn. Reson.*, **64**, 441 (1985).
4) J. Schaefer, R.A. McKay, and E.O. Stejskal, *J. Magn. Reson.*, **52**, 123 (1983).
5) J. Schaefer, E.O. Stejskal, D. Perchak, J. Skolnick, and R. Yaris, *Macromolecules*, **18**, 368 (1985).
6) M.D. Poliks and J. Schaefer, *Macromolecules*, **23**, 3426 (1990).
7) F. Horii, Y. Chen, M. Nakagawa, B. Gabrys, and R. Kitamaru, *Bull. Inst. Chem. Res., Kyoto Univ.*, **66**, 317 (1988).
8) T. Beppu, T. Murata, T. Uyeda, F. Horii, and H. Odani, *Polym. Prepr., Japan*, **40**, 3964 (1991).
9) T. Uyeda, F. Horii, H. Odani, T. Masuda, and T. Higashimura, *Polym. Prepr., Japan*, **40**, 1113 (1991).
10) A. Bax, N.M. Szeverenyi, and G.E. Maciel, *J. Magn. Reson.*, **55**, 494 (1983).

11) T. Terao, T. Fujii, T. Onodera, and A. Saika, *Chem. Phys. Lett.*, **107**, 145 (1984).
12) G. Bodenhausen, R. Freeman, and G.A. Morris, *J. Magn. Reson.*, **23**, 171 (1976).
13) G.A. Morris and R. Freeman, *J. Magn. Reson.*, **29**, 433 (1978).
14) K.T. Mueller, B.Q. Sun, G.C. Chingas, J.W. Zwanziger, T. Terao, and A. Pines, *J. Magn. Reson.*, **86**, 470 (1990).
15) J.H. Iwamiya, M.F. Davis, and G.E. Maciel, *J. Magn. Reson.*, **88**, 199 (1990).
16) M. Mehring, "Principles of High Resolution NMR in Solids", Springer-Verlag, Berlin, Heidelberg, and New York, 1983.
17) A. Abragam, "The Principles of Nuclear Magnetism", Oxford Univ. Press, London, 1961.
18) M.E. Rose, "Elementary Theory of Angular Momentum", John Wiley, New York, 1967.
19) Q.T. Pham, R. Petiand, H. Waton, and M.-F. Llouro-Darricades, "Proton and Carbon NMR Spectra of Polymers", Penton Press, London, 1991.